

Reactive Agent-based Model for Convergence of Autonomous Vehicles to Parallel Formations Heading to Predefined Directions of Motion

Vander L. S. Freitas¹ and Elbert E. N. Macau²

¹National Institute for Space Research - INPE, 12227-010, São José dos Campos, Brazil

²Laboratory of Computing and Applied Mathematics, National Institute for Space Research - INPE, 12227-010, São José dos Campos, Brazil

Keywords: Reactive Agents, Parallel Formation, Collective Motion.

Abstract: In this work we introduce a reactive agent-based model for convergence of autonomous vehicles to parallel formations heading to predefined directions of motion. They interact via rules of repulsion, alignment and attraction. There is also an abstraction of the desired path of motion, represented by a virtual guiding vehicle, which shows the desired direction to be followed by the formation. We performed simulations with different combinations of interaction rules and studied the parameter space. Additionally, we simulate the occurrence of communication failure among agents and the presence of noise. The resulting formations are evaluated by three quantifiers.

1 INTRODUCTION

Nature exhibits many emergent motions in collections of living beings. These emergent order behaviors are the result of local interactions among the agents. Common situations of the emergence of collective motion are in predator escaping, food search or hunting, for example.

Collective motion is a phenomenon that occurs in collections of agents, similar or not, who interact with each other, resulting in ordered motion (Vicsek and Zafeiris, 2012). Those interactions can be among close neighbors or in the context of a more evolved framework. Collective motion is present everywhere, from colonies of bacteria to schools of fish (Paley et al., 2007). There are about 1 million species of known insects in the world (Chapman et al., 2009) and despite most of them live lonely, many others are famous because of their organized behavior (Vicsek and Zafeiris, 2012).

The motivation for the study of collective motion is to understand the interaction rules among the units. These rules may be applied to artificial vehicles so they can work collaboratively in some tasks. Then it is possible to establish a link between control theory and applications of collective like robot swarms.

Studies on collective motion have resulted on models that attempt to recreate the observed collective arrangements of agents (Reynolds, 1987; Vicsek

et al., 1995; Czirók et al., 1999; Couzin et al., 2002; Paley, 2007; Cucker and Smale, 2007; Veerman et al., 2005; Dafflon et al., 2013). They are used in many applications like satellites in flight formation (Salazar, 2012), unmanned aerial vehicles (Klein, 2005) (Park et al., 2015), unmanned subaquatic vehicles (Leonard et al., 2007), aquatic surface robots (Duarte et al., 2016) and others.

In this work we propose a reactive agent-based model for convergence of autonomous vehicles to moving formations. The aim is to group the vehicles inside a moving bounded area heading to a predefined direction. The agents interact via rules of repulsion, alignment and attraction, similar to the works of Reynolds (Reynolds, 1987). The main difference is that here there is an individual called *virtual agent* (VA), i.e., a “virtual vehicle” that represents the desired path we want to be followed by the formation. It is not a real vehicle of the model but an abstraction. The individuals begin at random positions inside an area and after a transient of interactions they converge to a moving formation that heads in parallel to the same direction of motion of the VA.

The behavior of the virtual agent is similar to a leader, or the *stakeholder* agents of (Kerman et al., 2012), which have privileged information about the desired direction of the motion. The main difference is that, as mentioned before, it is not a real vehicle but an abstraction.

One possible usage of the VA would be to consider it as a moving GPS signal. In this case, one should expect the agents to converge in a parallel formation around its signal coordinates. Considering a scenario in which the vehicles are disperse in an environment and doing some work, e.g., measuring temperature, if one wants them to head to another geographic location, our model would be a good choice since VA dictates the path for the flock. Additionally, the model has the advantage of making the individuals getting together, which is useful to group disperse agents.

(Duarte et al., 2016) presented controls using neural networks and one of the tasks their aquatic robots can do is to go towards a geographic location. The role of our virtual agent is also to point out coordinates to be followed, but with the difference that these coordinates change through time.

The interaction rules have biological inspiration, derived from fishes and birds. (Herbert-Read et al., 2011) analyzed 2D trajectories of birds and observed rules of attraction and repulsion between close neighbors. In a similar work, (Katz et al., 2011) found out that fishes change their trajectories depending on the neighbors in front of them. In this work we present strategies for attraction and repulsion usage in the context of ordered motion.

We performed experiments in parameter space to seek for formations according to specific objectives. Besides, we simulated communication problems, by adding a probability distribution of individuals not responding to the environment stimuli on each time instant. Lastly, we verified the model behavior in the presence of a random noise. Both noise and communication failures have to be considered when designing real systems of this kind (Duarte et al., 2016), because the individuals have sensors with limited precision. Also, there are environmental issues like the presence of wind, for aquatic robots, or terrain irregularities for terrestrial vehicles, etc.

The paper is organized as follows. Section 2 details the reactive model, Section 3 presents implementation details, Section 4 reports some simulation results and Section 5 shows our conclusions.

2 REACTIVE MODEL

This model is called reactive because it uses the architecture of reactive agents, in which the individuals do not keep information of the past, but only respond to the current state of the system (Russell and Norvig, 2003).

The components of our proposed model are the so-called virtual agent, with its interaction radius, and

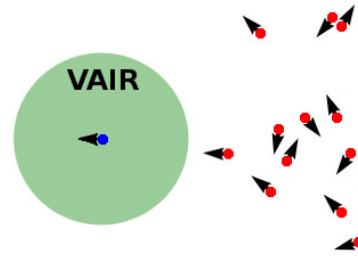


Figure 1: Model components: Virtual agent is in blue, agents are in red and VAIR is in green.

the reactive agents, as follows (Figure 1):

- **Virtual Agent:** Its role is to point out the desired motion direction and the moving region in which we want that the agents to form a parallel formation. Despite its interaction with agents, it is not a real agent but an abstraction.
- **Virtual Agent Interaction Radius (VAIR):** Circular region centered in VA, inside which the parallel formation will converge.
- **Reactive Agents:** The agents of the model. They model autonomous vehicles. Their main characteristic is that they do not keep memory of previous interactions, i.e., they respond to the current system state according to simple rules.

The aim here is to make the agents to enter the VAIR and follow the VA in a parallel formation. For this purpose they interact via adjustments in their velocity module (speed) and rules (interaction strengths) based on *repulsion*, *alignment* and *attraction*. We call these interaction rules as “virtual forces”. Here the concept of force is related to how the presence of the neighbors of an agent i can impose changes on its heading angle $\theta_i = \theta_i(t)$.

The speed adjustment is performed according to the position of the agent in relation to the VAIR. When an agent is outside the VAIR its speed is higher than when it is inside, because it needs to reach the VA. When an agent is entering the VAIR it suffers a deceleration according to Eq 1, so it can move along with the VA. The idea is to guarantee that the parallel formation will occur inside the VAIR.

$$|v_i| = |v_a| - \frac{(|v_{ini}| - |v_a|)(t - t_f)}{\Delta t_i} \quad (1)$$

so that v_i is the velocity of agent i , v_a is the velocity of the VA, v_{ini} is the velocity of agent i at the moment it started entering the VAIR, t is the current time, t_f is the time instant in which the acceleration will finish and Δt_i is the total time of this procedure.

In this equation $\Delta t_i = \bar{t} + rnd$, in which \bar{t} represents the approximate time for the agent to move from the

VAIR boundary to the VA's position, and rnd is a random number in the interval $rnd \in (-\gamma, \gamma)$. Here we used $\gamma \doteq \bar{t}$ to guarantee a homogeneous distribution of agents inside the VAIR.

When an agent is leaving the VAIR, its speed increases according to Eq 2. In this case, $|v_{out}|$ represents the maximum speed outside the VAIR.

$$|v_i| = |v_a| - \frac{(|v_{out}| - |v_{ini}|)(t - t_f)}{\Delta t_i} \quad (2)$$

We use five interaction rules to achieve the parallel formation in the desired direction of motion. The rules are written in the form of imposed *control actions*, or “forces”, as follows (Figure 2):

- F_a (Alignment): Orders the agent to align with the average heading angles of its neighbors.
- F_c (Cohesion): Orders the agent to go to the center of mass of its neighbors.
- F_{av} (Alignment with virtual agent): Orders the agent to align with the VA heading angle.
- F_{cv} (Cohesion with virtual agent): Orders the agent to move towards the VA.
- F_s (Separation): Orders the agent to move apart from its nearest neighbor.

All of those *control actions* are applied to the agent as the angular velocity control input, acting directly on the heading angle of the agents at discrete time. Their maximum value is 1.00 decimal degree per time unit to account for limitations that may be present in the heading angle changes of real robots. For example, if agent 1 has $\theta_1 = 150.00$ as its heading angle, and VA $\theta_a = 160.00$, when F_a is applied it will result in $F_a = 1.00$ and $\theta_1 = 151.00$. However, if $\theta_1 = 159.50$ and $\theta_a = 160.00$ and F_a is applied, the result would be $F_a = 0.50$ and consequently $\theta_1 = 160.00$. Each time unit (tu) corresponds to a travel of 1.00 bl (body length of an agent) of VA, i.e., the VA's speed is $|v_a| = 1 bl/tu$.

F_a and F_c do the same than alignment and cohesion rules defined by Reynolds (Reynolds, 1987). Each isolated force produces an effect but we are interested on the combinations of them. For this case the resulting force F is calculated as a linear combination of the five forces, according to Eq 3.

$$F(t) = \frac{\alpha_a F_a(t) + \alpha_c F_c(t) + \alpha_{av} F_{av}(t) + \alpha_{cv} F_{cv}(t)}{\alpha_a + \alpha_c + \alpha_{av} + \alpha_{cv}} \quad (3)$$

in which α_a , α_c , α_{av} , α_{cv} are control coefficients and each force is unitary. The separation force does not appear here because it is used isolated when a collision between two individuals is about to happen. In this case, we use Eq 4.

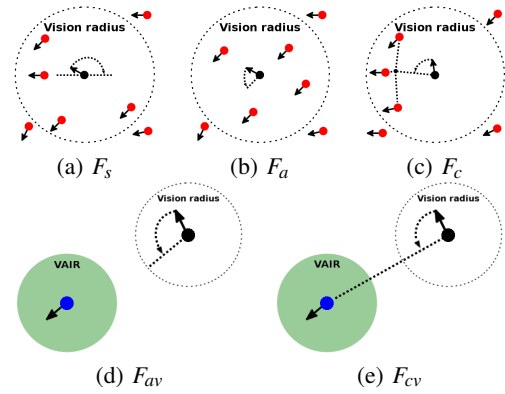


Figure 2: Interaction rules. The dotted circumferences represent the interaction area (vision radius) of one agent (in black). At (d) and (e) the blue agent is the virtual agent.

$$F(t) = F_s(t) \quad (4)$$

The dynamics of an agent is given by Eq 5.

$$\begin{aligned} \dot{x}_i &= |v_i| \cdot \cos(\theta_i) \\ \dot{y}_i &= |v_i| \cdot \sin(\theta_i) \\ \dot{\theta}_i &= F \end{aligned} \quad (5)$$

where $[x_i, y_i]^T \in \mathbb{R}^2$ is the i th agent's position, expressed in terms of polar coordinates.

The virtual agent represents the desired trajectory for the parallel formation, i.e., the position over time that we want our formation to follow. Its dynamics works as an ordinary agent but with fixed heading angle θ_i , velocity $|v_i| = |v_a|$.

3 IMPLEMENTATION

The simulations were implemented using the Python language and some libraries like matplotlib¹ and numpy², for plotting, random number generation, etc.

The simulation scenario works as a torus. When the agents reach the outskirts of the environment, they appear at the opposite side, heading to the same direction as before. For example, when they are heading to the left and cross the limits they appear at right.

Agents begin in a bounded rectangular area behind the VA, with random coordinates and heading angles as shown in Figure 1. The coordinate system is given by the size of the agent. We assumed that the VA is able to move the distance of one body length (bl) per time unit (tu). Considering that particles have a circular shape, this bl is their diameter.

The implementation has basically three classes: Agent, Model and Simulation. Agent represents each

¹<http://matplotlib.org/>

²<http://www.numpy.org/>

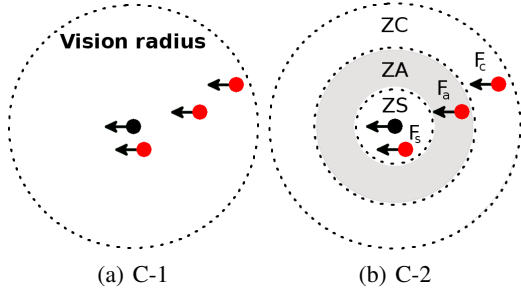


Figure 3: Calculation of forces: S-1) Considering the entire agent vision radius equally; and S-2) Considering zones of perception (ZS - Zone of separation, ZA - Zone of alignment and ZC - Zone of cohesion). The black agent is an ordinary agent of the model and the dotted region corresponds to its vision region (perception region). Agents in red are its neighbors.

agent of the simulation, with its coordinates and speed. When the agent enters or leaves the VAIR, its speed changes through Eqs. 1 and 2. The class Model has a list of agents and is responsible for evolving the model, according to the Eq. 5, parameters like neighborhood radius, control coefficients $\alpha_a, \alpha_c, \alpha_{av}, \alpha_{cv}$, and the chosen strategy. The strategies are presented in the next section. The class Simulation is responsible for setting up the parameters of the model and running the simulations.

4 RESULTS

There are two approaches to deal with the neighborhood of each agent. In the first (S-1) the agent considers a neighborhood radius in which every neighbor is treated similarly, i.e., the control actions (forces) are applied without distinction, regarding their position (Figure 3a).

The second approach (S-2) takes into account the distances between the agent and its neighbors through perception zones (Figure 3b). In this case, when a neighbor is in the first radius, closer to the agent, only F_s is calculated. Following the same logic, when the neighbor is in the second zone (ZA), only the force of alignment F_a is computed, and in the third zone (ZC), only F_c is considered. This approach is inspired in an observed behavior that occurs in schools of fish. (Katz et al., 2011) showed that some species of fish increase their speed when a neighbor is far ahead (attraction), while decreases when it is too close (separation). (Kerman et al., 2012) has implemented these three perception zones but the outer region (ZC) contains the other two inside, and ZA contains ZS. Here we consider them as rings, i.e., they do not overlap, similar to the works of (Couzin et al., 2002).

We test four strategies (combinations of forces) as shown in Table 1. The application of forces depends on whether the agent is inside or outside the VAIR. Despite there are only four strategies, the table shows eight possibilities because of the two approaches of neighborhood calculation, S-1 and S-2.

Table 1: Strategies (combinations of control actions) used when the agents are inside or outside the VAIR.

| Strategy | Outside the VAIR | Inside the VAIR |
|---------------|----------------------------|-----------------|
| S-1.1 (S-2.1) | F_a, F_{cv} | F_{av} |
| S-1.2 (S-2.2) | F_{cv} | F_{av}, F_a |
| S-1.3 (S-2.3) | F_{cv}, F_c | F_{av}, F_a |
| S-1.4 (S-2.4) | F_{cv}, F_c, F_{av}, F_a | F_{av}, F_a |

Definition 1 *If all agents are moving in a parallel formation inside the VAIR and have the same speed of the virtual agent, then they are in a Desired Formation (DF).*

We consider they are in parallel if the higher difference between the VA heading angle θ_a and each agent heading angle θ_i is smaller than an imposed tolerance β_{lim} . In other words, they are in parallel if $|\theta_a - \theta_i| < \beta_{lim}$, for $i \in \{1, 2, \dots, N\}$.

We define three quantifiers to measure what kind of parallel formations we can get with different combinations of control actions:

1. Temporal index (τ): time units (tu) from the beginning of the simulation until the DF.
2. Angular uniformity index (ϕ): The relative angles between the position of each agent and the VA is calculated. Then the order parameter (Eq 6 - (Strogatz, 2000)) is evaluated with those angles.

$$p_\Theta \doteq \frac{1}{N} \sum_{j=1}^N e^{i\Theta_j} \quad (6)$$

with $e^{i\Theta_k} = \cos \Theta_j + i \sin \Theta_j$.

In this case, $\phi = |p_\Theta|$. When $\phi = 0$ the agents are uniformly distributed around the VA. On the other hand, if $\phi = 1$ then the agents are at the same position.

3. Radial uniformity index (ρ): The mean of the distances between each agent and the VA.

The first index (τ) computes the total time for the model convergence, and the two others, ϕ and ρ , are related to the distribution of the formation. If the agents are very close to each other, they have small ρ . For the case in which the agents converge to straight lines, following the VA, ϕ is near 1. On the other hand, when the agents converge to some sort of circular shape, centered in VA, ϕ is close to zero.

We evaluated the strategies with all combinations of $\alpha_a, \alpha_c, \alpha_{av}, \alpha_{cv} \in \{1, 2, \dots, 10\}$. Each configuration is simulated 10 times using random initial positions and heading angles $\theta = (\theta_i(t))_{i=1,2,\dots,N}$.

Initial conditions:

- Population of $N = 12$ agents randomly positioned inside a rectangle of dimensions $36 \times 76 \text{ bl}$, as shown in Figure 1.
- Vision radius of each agent: 5.5 bl .
- Minimum separation: 2.5 bl .
- F_s : 2 decimal degrees.
- $F_a = F_c = F_{av} = F_{cv}$: 1 decimal degree.
- Heading angles θ : Random.
- $|v_a| = 1 \text{ bl/tu}$, $|v_{out}| = 1.4 \text{ bl/tu}$.
- VAIR: 25 bl .
- Virtual agent heading angle: 180 decimal degrees.
- β_{lim} : 5 decimal degrees.

Only cases that reach the DF for all 10 attempts and obeying $\tau \leq 3000 \text{ tu}$ are considered. Simulations are limited to this temporal limit of 3000 tu due to the large number of combinations in parameter space. Also, this value is set because the agents usually converge in less than 2000 tu , according to experimental observations.

We calculate the three indexes for each combination of control coefficients. Figure 4 depicts the desired formations achieved in terms of the maximum and minimum values of τ , ϕ and ρ .

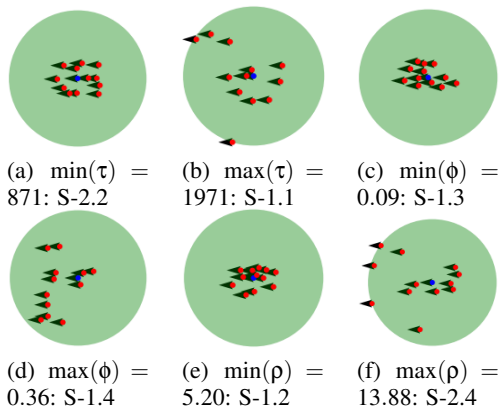


Figure 4: Desired formations for the simulated configurations in terms of the maximum and minimum values achieved for τ , ϕ and ρ . Configurations: (a) S-2.2: $\alpha_a = 8$, $\alpha_{av} = 9$ and $\alpha_{cv} = 4$; (b) S-1.1: $\alpha_a = 7$, $\alpha_{av} = 1$ and $\alpha_{cv} = 3$; (c) S-1.3: $\alpha_a = 1$, $\alpha_c = 4$, $\alpha_{av} = 4$ and $\alpha_{cv} = 9$; (d) S-1.4: $\alpha_a = 3$, $\alpha_c = 5$, $\alpha_{av} = 7$ and $\alpha_{cv} = 9$; (e) S-1.2: $\alpha_a = 3$, $\alpha_{av} = 10$ and $\alpha_{cv} = 10$; (f) S-2.4: $\alpha_a = 2$, $\alpha_c = 3$, $\alpha_{av} = 6$ and $\alpha_{cv} = 9$.

If one wants agents to converge as fast as possible, a good choice would be strategy S-2.2 with the configuration of Figure 4a. An example of simulation with this configuration is shown in Figure 5. Otherwise, if the aim is to get them very close to each other the best option is the configuration of strategy S-1.2 of Figure 4e. The resulting formations depends on both the chosen strategy and configuration. In this sense, some strategies are more suitable for some objectives than others.

In a situation in which one desires the agents to spread uniformly inside the VAIR, ϕ would be near zero and ρ around the half of VAIR size. Considering an application in which surveillance vehicles are monitoring an area it is expected that they travel far from each other, so they can explore a bigger area. For this purpose, ρ should be as large as possible.

Certain combinations of parameters α do not lead to the expected convergence. If one sets the α_a value much higher than α_{av} , it is possible that the agents never follow the VA because they are more likely to converge to a parallel motion heading elsewhere. Figure 6 shows the dependence between α_a and α_{av} for strategy S-2.2, in which the colors correspond to the rate of DF convergence. The agents are more likely to reach the DF when $\alpha_{av} \geq \alpha_a$, for S-2.2.

We simulate failures on communication, emulating what would happen case an agent lost the feedback from its neighbors during a time unit. In our setup, this problem does not last until the end of the simulation, but it is calculated each time unit. Also, we add a random noise to the dynamics of their heading angles, to simulate external interferences from the environment (wind, terrain irregularities, etc) and sensor imprecisions.

The random noise $\epsilon \in [-\delta, \delta]$ is applied according to Eq. 7, with δ representing the noise strength. There is also a probability p of the agent to ignore its neighbors stimuli. We simulate both noise and communication failure for each agent, independently, to account for what would happen in a real world system.

$$\dot{\theta} = F + \epsilon \quad (7)$$

We have chosen strategy S-2.2 with the configuration of Figure 4a to simulate noise and communication failures, because it converges faster than the others.

We varied $p \in [0, 0.9]$ and $\delta \in [0, 0.9]$, with steps of $\Delta p = \Delta \delta = 0.1$, and calculated the average of 50 simulations for each pair (p, δ) since initial conditions are random. Figure 7a shows the results. Seems like for $p \in [0, 0.8]$ there is no change in the colors, because of the abrupt difference between $p = 0.8$ and $p = 0.9$. Figure 7b presents this region in more de-

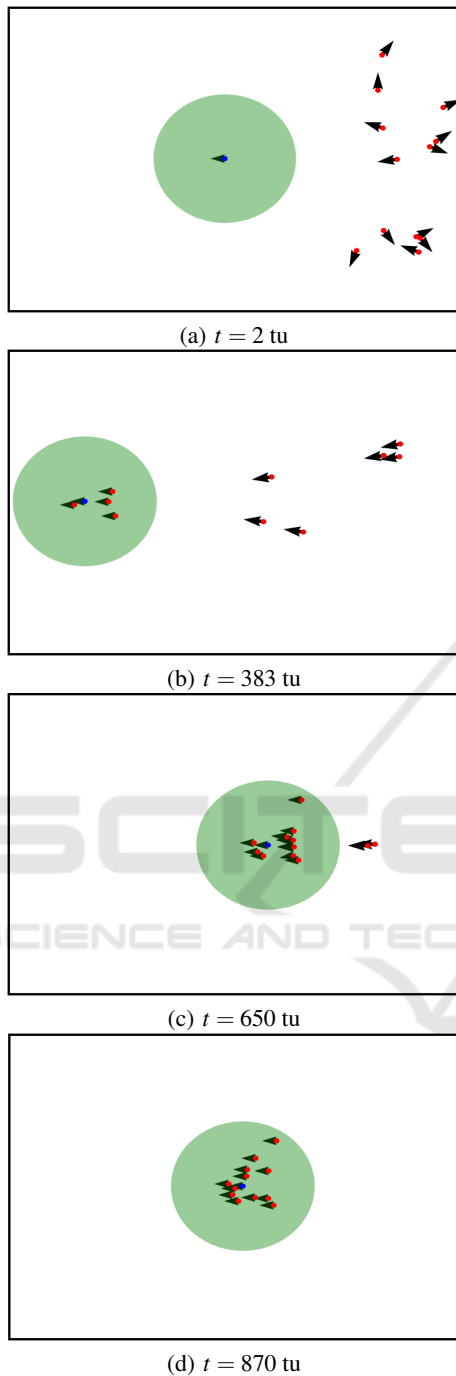


Figure 5: Simulation of strategy S-2.2 with configuration $\alpha_a = 8$, $\alpha_{av} = 9$ and $\alpha_{cv} = 4$.

tails. As expected, the higher the value of p the longer it takes to reach the desired formation, with τ increasing smoothly for $p \in [0, 0.8]$. When $p = 0.9$ it suddenly jumps to a very high value. It probably happened because for S-2.2 the only force acting outside the VAIR is F_{cv} . If the agents ignore it with a probability of $p = 0.9$, then they will only try to go towards

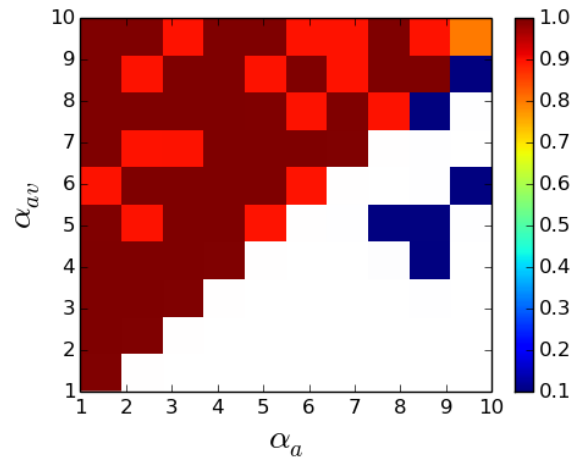


Figure 6: Convergence ratio when varying control coefficients α_a and α_{av} for strategy S-2.2. Colors represent the convergence ratio and white regions represent the cases in which DF was not achieved. The agents are more likely to reach the DF when $\alpha_{av} \geq \alpha_a$.

VA 10% of the cases, resulting in a very high τ .

The values of ϵ were proportional to θ and it seems like ϵ does not affect the convergence of formations, according to Figure 7.

Results have shown that this model is quite resilient to communication failures, and the presence of noise, since their impact was small, specially for noise.

5 CONCLUSIONS

We presented a reactive agent-based model whose aim is to make agents converge to parallel formations heading to a desired direction. We introduced the so-called virtual agent, whose role is to indicate the formations direction of motion and also to evaluate their shapes. The agents interact via five rules depending on a chosen strategy (combination of rules) and a configuration (weight of each rule).

Four strategies were evaluated and analyzed for about 44,000 configurations, considering two neighborhood approaches to calculate the virtual forces: one taking into account the presence of neighbors likewise, and the other using non-overlapping interaction zones.

The last simulations were focused on communication failures, in which the agents had a probability of ignoring the external stimuli from neighbors, each time unit. This represents failures on the wireless network, or even the GPS signal. Besides, we added a random additive noise to the agents heading angle, to account for the sensors imprecision, and environmen-

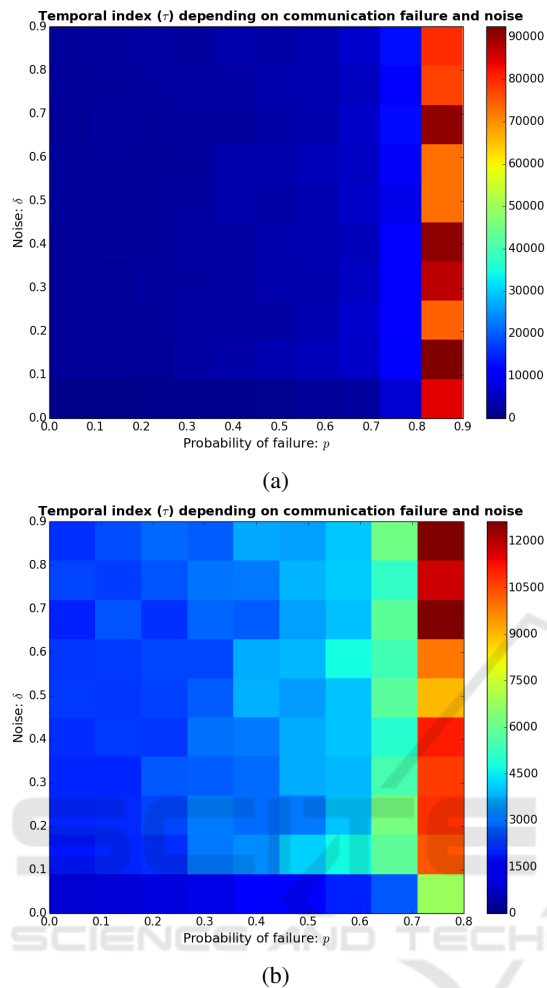


Figure 7: Temporal index (τ) depending on the probability of communication failure p and a random noise $\epsilon \in [-\delta, \delta]$, for S-2.2, with $\alpha_a = 8$, $\alpha_{av} = 9$ and $\alpha_{cv} = 4$. (a) communication failure with $p \in [0, 0.9]$, (b) Zooming to $p \in [0, 0.8]$. Color represents τ .

tal issues as the presence of wind or terrain irregularities. Results have shown that our model is quite resilient to communication failures, and the presence of noise, since their impact was small, specially for noise.

Considering that agents have sensory limitations, one can use this model as a pre-step before switching to another model with more controls, since its principle is to group agents into a bounded region.

ACKNOWLEDGEMENTS

The authors would like to thank the Conselho Nacional de Desenvolvimento Científico e Tecnológico - CNPq, and the Coordenacao de Aperfeiçoamento

de Pessoal de Nivel Superior - CAPES, for the financial support. EENM thanks FAPESP, processes 2011/50151-0 and 2015/50122-0, and CNPq, process 458070/2014-9, for their support.

REFERENCES

- Chapman, A. D., Study, A. B. R., and Australia. (2009). *Numbers of living species in Australia and the world / Arthur D. Chapman*. Department of the Environment, Water, Heritage and the Arts [Canberra, ACT].
- Couzin, I. D., Krause, J., James, R., Ruxton, G. D., and Franks, N. R. (2002). Collective memory and spatial sorting in animal groups. *Journal of Theoretical Biology*, 218(1):1 – 11.
- Cucker, F. and Smale, S. (2007). Emergent behavior in flocks. *IEEE Transactions on Automatic Control*, pages 852–862.
- Czirók, A., Barabási, A.-L., and Vicsek, T. (1999). Collective motion of self-propelled particles: Kinetic phase transition in one dimension. *Phys. Rev. Lett.*, 82:209–212.
- Dafflon, B., Gechter, F., Gruer, P., and Koukam, A. (2013). Vehicle platoon and obstacle avoidance: A reactive agent approach. *IET Intelligent Transport Systems*, 7(3):257–264.
- Duarte, M., Costa, V., Gomes, J., Rodrigues, T., Silva, F., Oliveira, S. M., and Christensen, A. L. (2016). Evolution of collective behaviors for a real swarm of aquatic surface robots. *PLOS ONE*, 11(3):1–25.
- Herbert-Read, J. E., Perna, A., Mann, R. P., Schaerf, T. M., Sumpter, D. J. T., and Ward, A. J. W. (2011). Inferring the rules of interaction of shoaling fish. *Proceedings of the National Academy of Sciences*, 108(46):18726–18731.
- Katz, Y., Tunstrom, K., Ioannou, C. C., Huepe, C., and Couzin, I. D. (2011). Inferring the structure and dynamics of interactions in schooling fish. *Proceedings of the National Academy of Sciences*, 108(46):18720–18725.
- Kerman, S., Brown, D., and Goodrich, M. A. (2012). Supporting human interaction with robust robot swarms. In *Resilient Control Systems (ISRCS), 2012 5th International Symposium on*, pages 197–202.
- Klein, J. K. (2005). Controlled Collective Motion for Multivehicle Trajectory Tracking. Master’s thesis, University of Washington, USA.
- Leonard, N., Paley, D., Lekien, F., Sepulchre, R., Fratantonio, D., and Davis, R. (2007). Collective motion, sensor networks, and ocean sampling. *Proceedings of the IEEE*, 95(1):48–74.
- Paley, D., Leonard, N. E., Sepulchre, R., Grünbaum, D., and Parrish, J. K. (2007). Oscillator models and collective motion: Spatial patterns in the dynamics of engineered and biological networks. *IEEE Control Systems Magazine*, 27(4):89–105.
- Paley, D. A. (2007). *Cooperative control of collective motion for ocean sampling with autonomous vehicles*. PhD thesis, Princeton University.

- Park, C., Cho, N., Lee, K., and Kim, Y. (2015). Formation flight of multiple uavs via onboard sensor information sharing. *Sensors*, 15:17397–17419.
- Reynolds, C. W. (1987). Flocks, herds and schools: A distributed behavioral model. *SIGGRAPH Comput. Graph.*, 21(4):25–34.
- Russell, S. J. and Norvig, P. (2003). *Artificial Intelligence*. Pearson Education, 2 edition.
- Salazar, F. J. T. (2012). *Deployment and maintenance of a satellite formation flight around L4 and L5 lagrangian points in the earth-moon system based on low cost strategies*. PhD thesis, Instituto Nacional de Pesquisas Espaciais.
- Strogatz, S. H. (2000). From kuramoto to crawford: Exploring the onset of synchronization in populations of coupled oscillators. *Phys. D*, 143(1-4):1–20.
- Veerman, J. J. P., Lafferriere, G., Caughman, J. S., and Williams, A. (2005). Flocks and formations. *Journal of Statistical Physics*, 121(5):901–936.
- Vicsek, T., Czirók, A., Ben-Jacob, E., Cohen, I., and Shochet, O. (1995). Novel type of phase transition in a system of self-driven particles. *Phys. Rev. Lett.*, 75:1226–1229.
- Vicsek, T. and Zafeiris, A. (2012). Collective motion. *Physics Reports*, 517(3-4):71 – 140. Collective motion.

